

Magnetic field dependence of the spin dynamics in the reentrant spin glass $\text{Fe}_{70.4}\text{Al}_{29.6}$

P. Böni and S. M. Shapiro

Brookhaven National Laboratory, Upton, New York 11973-5000

K. Motoya

Department of Physics, Faculty of Science, Saitama University, 255 Shimo-Okubo, Urawa, Saitama 338, Japan

(Received 15 July 1987)

The field dependence of the inelastic neutron scattering from the reentrant spin glass (RSG) $\text{Fe}_{70.4}\text{Al}_{29.6}$ is investigated below T_C . In the intermediate paramagnetic phase $100 \text{ K} < T < T_c^{\text{inv}} \simeq 200 \text{ K}$ spin waves are induced in an applied field. The peaks broaden rapidly with increasing q and decreasing temperature. Remarkably these excitations exhibit a dispersion curve with a "negative" slope. In a field of 10 kOe the energy gap corresponds to a Zeeman splitting $g\mu_B H \simeq 0.11 \text{ meV}$. In the spin-glass phase at 10 K no inelastic scattering is observed in a field, although the sample is close to saturation. The results are interpreted in terms of a field-induced dispersion, which has been observed recently in a diluted random antiferromagnet.

I. INTRODUCTION

The properties of spin glasses have been studied in the past in numerous experimental and theoretical work.^{1,2} The statics and the dynamics are, however, still far from being well understood. It is not even clear if the transitions which lead to the spin-glass phase are real equilibrium phase transitions.^{3,4} A schematic picture of a spin glass is that of a frozen paramagnet. The spins point in random directions because of frustration which can be caused by competing types of interactions, for example, Ruderman-Kittel-Kasuya-Yosida (RKKY) interactions, exchange interactions, or random anisotropy, to name only a few. Therefore it is not astonishing that there exists a whole variety of spin glasses which exhibit a wide variety of magnetic properties.

A class of spin glasses that has generated a large interest are those called reentrant spin glasses (RSG). These systems exhibit an unusual sequence of transitions: In the high-temperature state they are paramagnetic and at some well-defined critical temperature T_C they undergo a transition to a ferromagnetic-like state. At a still lower temperature the system exhibits spin-glass-like properties. The physical nature of this state is not clear and theories suggest that the RSG state is really composed of a mixed state exhibiting ferromagnetic and spin-glass behavior.⁵

The magnetic properties of the RSG $\text{Fe}_x\text{Al}_{1-x}$ with $x=0.3$ were investigated recently in detail by means of neutron scattering techniques. Measurements of Cable *et al.*⁶ indicate the presence of ferromagnetic clusters over the entire temperature range below T_C . Child⁷ extended the former measurements to smaller q and found that the magnetic scattering was very sensitive to external magnetic fields. Motoya *et al.*⁸ probed, in addition, the inelastic scattering from $\text{Fe}_{70}\text{Al}_{30}$. They observed a peculiar sequence of phase transitions as shown in Fig. 1 for the present sample. Below the Curie temperature T_C

($\simeq 550 \text{ K}$), the sample exhibits long-range ferromagnetic order and one observes spin waves as shown for $T=350 \text{ K}$. In contrast to a normal ferromagnet, the spin waves start to soften around 300 K with decreasing temperature (see $T=250 \text{ K}$). Below $T_c^{\text{inv}} \simeq 200 \text{ K}$ the system enters again a paramagnetic-like state and the scattering is quasielastic with a large intensity at $E=0 \text{ meV}$. Finally, below $T \simeq 90 \text{ K}$, the energy width of the scattering becomes resolution limited and the peak becomes very intense when the system enters a spin-glass state. This behavior differs from that recently reported by Hennion *et al.*⁹ on Ni-Mn, where they see an increase in the spin-wave energy at the lowest temperatures.

Only little attention has been given until now to the field dependence of the magnetic correlation in RSG. Several groups have recently investigated amorphous RSG and observed a rapid decrease of the small-angle intensity with increasing field and hysteretic behavior.¹⁰⁻¹³ Shapiro *et al.*¹⁴ observed the appearance of spin waves in the spin-glass phase of $\text{Fe}_x\text{Cr}_{1-x}$ upon applying a field, indicating an induced ferromagnetic state. Very recently Böni *et al.*¹⁵ studied the magnetic field dependence of the elastic scattering from a single crystal $\text{Fe}_{70.4}\text{Al}_{29.6}$ (the present sample). Surprisingly, they observed the appearance of a peak at finite momentum q suggesting a field-induced, modulated spin structure (see Fig. 2) for q parallel and perpendicular to the field. Similar observations were made by Hennion *et al.*¹⁶ in the polycrystalline RSG $\text{Ni}_{1-x}\text{Mn}_x$ and $\text{Au}_{1-x}\text{Fe}_x$, and in the amorphous $(\text{Fe}_{1-x}\text{Mn}_x)_{75}\text{P}_{16}\text{B}_6\text{Al}_3$. They pointed out that their results give evidence for the existence of frozen transverse-spin components as predicted by Gabay and Toulouse.⁵

We report in this paper on the field dependence of the inelastic neutron scattering from $\text{Fe}_{70.4}\text{Al}_{29.6}$, in order to answer the question if ferromagnetism can be restored in the spin-glass phase of $\text{Fe}_{70.4}\text{Al}_{29.6}$, and therefore to better understand the ground-state properties of RSG.

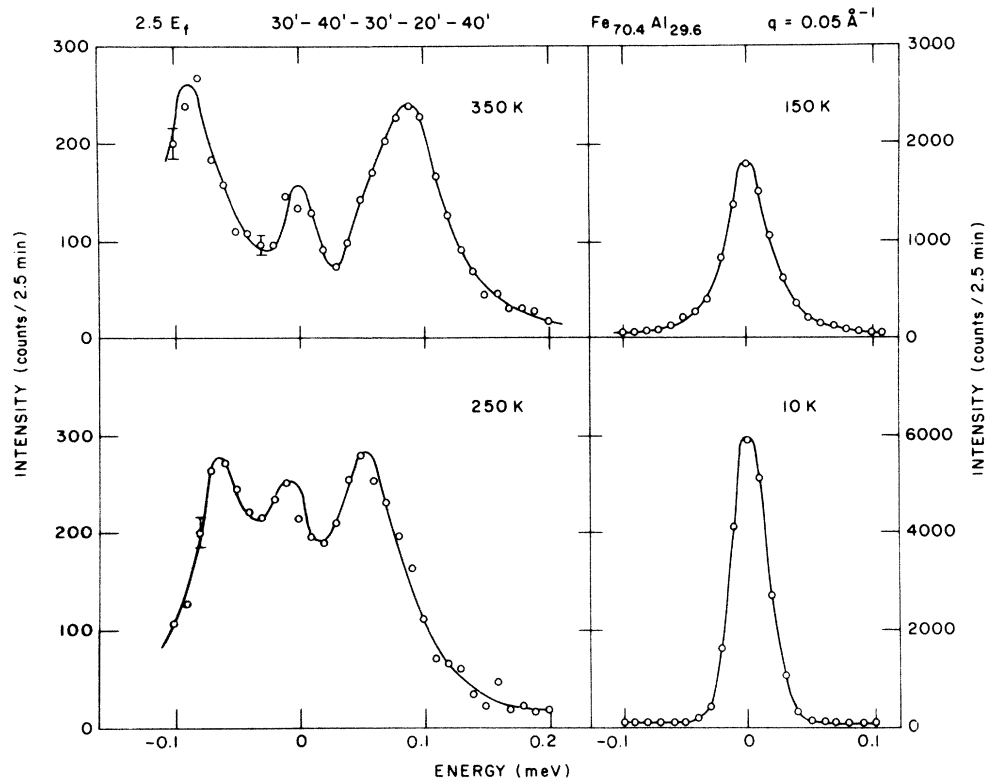


FIG. 1. Temperature dependence of the energy spectra in zero field measured for $q = 0.05 \text{ \AA}^{-1}$. Solid lines are fits to $S_L(Q, E)$.

Fe_{70.4}Al_{29.6} 5K

II. EXPERIMENT

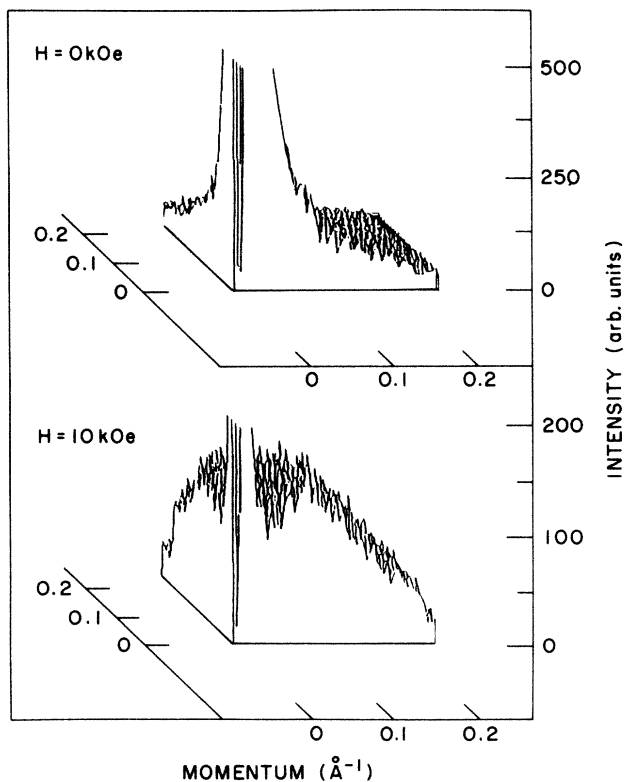


FIG. 2. SANS contours measured in the spin-glass phase at 10 K in a field of 10 kOe.

The composition of the present sample Fe_{70.4}Al_{29.6} is slightly at the more Fe-rich side than the sample used by Motoya *et al.*⁸ Therefore the present sample shows more pronounced ferromagnetic properties than the previous one. It exhibits FeAl type order, i.e., all cubic corner sites are occupied by Fe atoms, and the body-centered sites are randomly occupied by Fe or Al atoms. The lattice constant at room temperature is $a = 2.89 \text{ \AA}$.

The inelastic neutron scattering experiments were performed on a triple axis spectrometer at the cold source of the High Flux Beam Reactor at Brookhaven National Laboratory. The single-crystal sample was mounted with the [110] direction vertical. For the horizontal field (HF) measurements (\mathbf{H} parallel to \mathbf{Q}) the sample was mounted in a diplex cryostat positioned between the pole pieces of a water-cooled electromagnet. The vertical fields (VF) (with \mathbf{Q} perpendicular to \mathbf{H}) were applied by a superconducting coil with the sample mounted on the cold finger of a flow Dewar. The data were collected in the forward direction keeping fixed the final neutron energy at $E_f = 2.5$ or 2.6 meV . Pyrolytic graphite crystals set for the (002) reflection were used for the double monochromator and the analyzer. Higher-order neutrons were removed by a cooled beryllium filter. Various collimations were used depending upon the conflicting requirements of energy resolution and reasonable intensity. The half width at half maximum (HWHM) of the energy resolution was typically $15 \mu\text{eV}$.

III. MAGNETIC SCATTERING

The magnetic cross section for magnetic scattering can be written¹⁷

$$\frac{d^2\sigma}{d\Omega dE} = \gamma_0^2 \frac{k_f}{k_i} F(Q)^2 S(Q, E) e^{-2W}, \quad (1)$$

where $\gamma_0^2 = 0.291$ b is a constant, $F(Q)$ is the magnetic form factor, e^{-2W} is the Debye-Waller factor, and k_i and k_f are the wave vectors of the incident and scattered neutrons, respectively. Since there is no single correct form for $S(Q, E)$ available, we have used two different forms for $S(Q, E)$. In one case we choose a double Lorentzian form of the scattering function

$$S_L(Q, E) = \frac{A_s}{q^2} \frac{1}{2\pi} \left[\frac{\Gamma}{(E - E_q)^2 + \Gamma^2} + \frac{\Gamma}{(E + E_q)^2 + \Gamma^2} \right] \times \frac{E/k_B T}{1 - e^{-E/k_B T}} + \frac{A_G}{q^2} \delta(E), \quad (2)$$

where E_q represents the peak position of the spectra and Γ is the HWHM. The other form is the damped harmonic oscillator function

$$S_{DHO}(Q, E) = \frac{A_s}{q^2} \frac{1}{\pi} \frac{2\beta_q E_q^2}{(E^2 - E_q^2)^2 + 4\beta_q^2 E^2} \frac{E/k_B T}{1 - e^{-E/k_B T}} + \frac{A_G}{q^2} \delta(E). \quad (3)$$

In the latter form the eigenfrequency E_q is not necessarily equivalent with the maximum of $S(Q, E)$. Both forms were convoluted with the resolution function of the spectrometer and the appropriate parameters adjusted to give a best fit (smallest χ^2) to the observed data. Equation (2) is equivalent to Eq. (3) if $\Gamma \ll E_q$, then $\Gamma = \beta_q$. In order to take the elastic scattering around $E = 0$ into account we have added an additional q -dependent term which includes a δ function. A_s and A_G are normalization constants for the inelastic and elastic scattering, respectively, and q is the momentum transfer with respect to the Bragg peak. Since we performed all inelastic scans around the forward direction (the first Brillouin zone) $q = Q$ and $F(Q) \simeq 1$.

In Fig. 3 we summarize the results of the analysis of our zero-field data of Fig. 1 measured at 250 and 350 K using $S(Q, E)$ from Eq. (2). In the ferromagnetic regime $\Gamma \sim q^4 \ln^2(k_B T/E)$ and $E = Dq^2 + \Delta$, as expected for a Heisenberg ferromagnet. The stiffness constant D in the present sample is more than an order of magnitude smaller than in bcc iron,¹⁸ where $D = 281$ meV \AA^2 ($T = 300$ K), but larger than in the sample from Ref. 8, because of the higher Fe concentration. It is clearly seen that as the temperature decreases, D decreases. Also, a small gap $\Delta \simeq 0.03$ meV is present, which is temperature independent in this region.

Figure 4 shows that the spin-wave peaks are shifted to larger energies when a horizontal magnetic field HF is applied. The shift is, however, not proportional to H as expected for a simple Zeeman splitting (see inset of Fig.

4). Since the ferromagnetic state is believed to be a domain state we do not expect to observe a linear relation between E and H , because H may affect the exchange interactions as well by the increase of the domain sizes.

In Fig. 5 we show the temperature dependence of the magnetic scattering in a horizontal field of 10 kOe. If we compare it with the zero-field spectrum at $T = 150$ K we see that the quasielastic scattering has disappeared and we observe inelastic scattering which peaks at finite energy. The peaks broaden and their intensity decreases with decreasing temperature. At 10 K they have vanished completely and no inelastic scattering is visible at all. The elastic scattering, on the other hand, increases with decreasing temperature by more than an order of magnitude but the intensity is much less than in zero field.

The vertical field dependence of the magnetic scattering for $q = 0.043$ \AA^{-1} is depicted in Fig. 6 for $T = 150$ K. In zero field the scattering peaks at 0 meV (Fig. 1). The peaks move to higher energy with increasing field. At 20 kOe the peaks lie outside the spectrometer window because the momentum- and energy-conservation

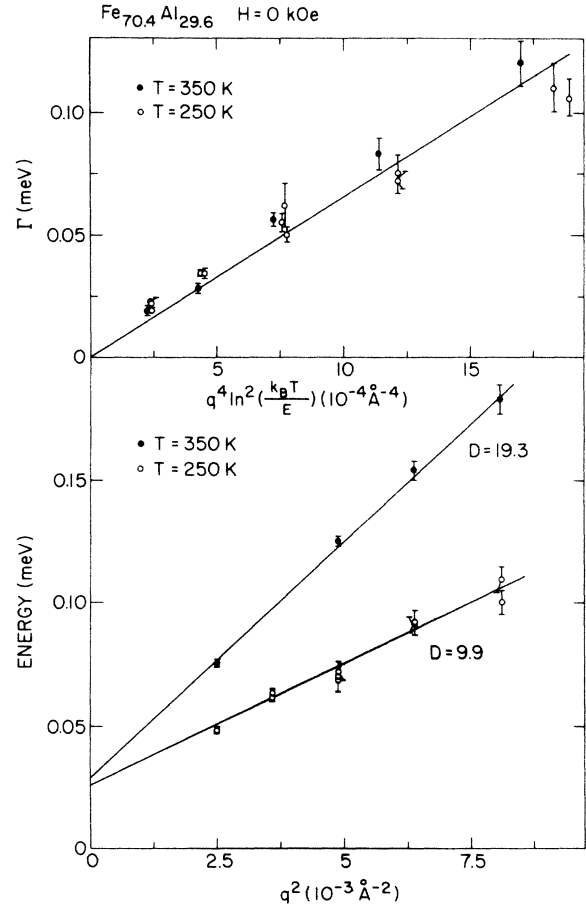


FIG. 3. Spin-wave widths and energies plotted as a function of $q^4 \ln^2(k_B T/E_q)$ and q^2 , respectively, measured for two different temperatures. Note the softening of the spin waves with decreasing temperature, in contrast to the behavior expected for a normal ferromagnet.

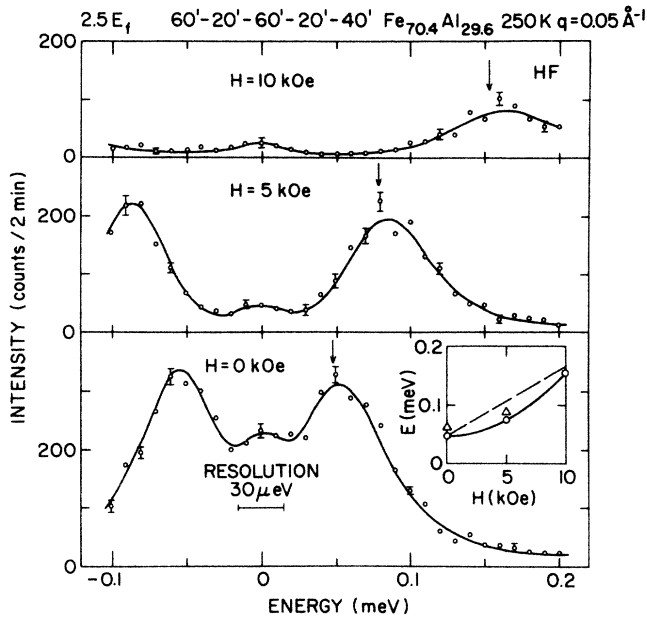


FIG. 4. Field dependence (HF) of the spin-wave energy at $T=250$ K and $q=0.05 \text{ \AA}^{-1}$. The solid lines represent fits to $S_L(Q,E)$ convoluted with the resolution function. The arrows indicate the peak positions of the deconvoluted cross section. The inset shows that the energy does not increase linearly (dashed line) with field, as expected for a normal ferromagnet. The circles represent measurements of 0.05 \AA^{-1} and the triangles measurements at 0.06 \AA^{-1} . The solid line is a guide to the eye.

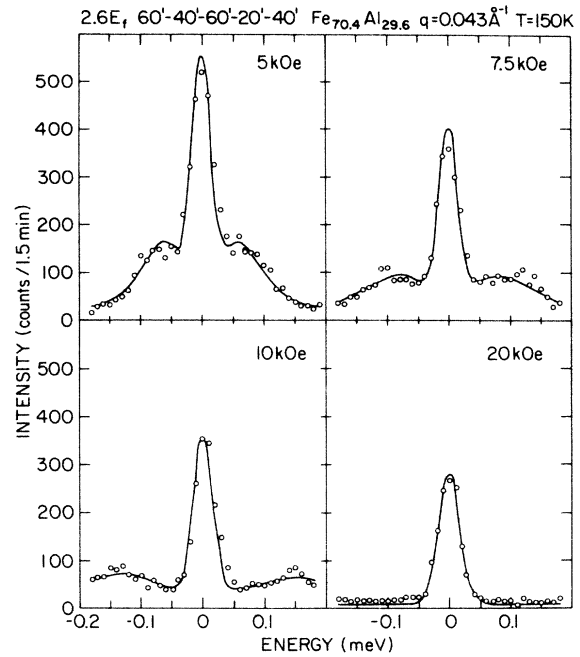


FIG. 6. Vertical field dependence of the inelastic scattering at $q=0.043 \text{ \AA}^{-1}$ measured in the intermediate paramagnetic phase at $T=150$ K. Solid lines are fits to $S_L(Q,E)$.

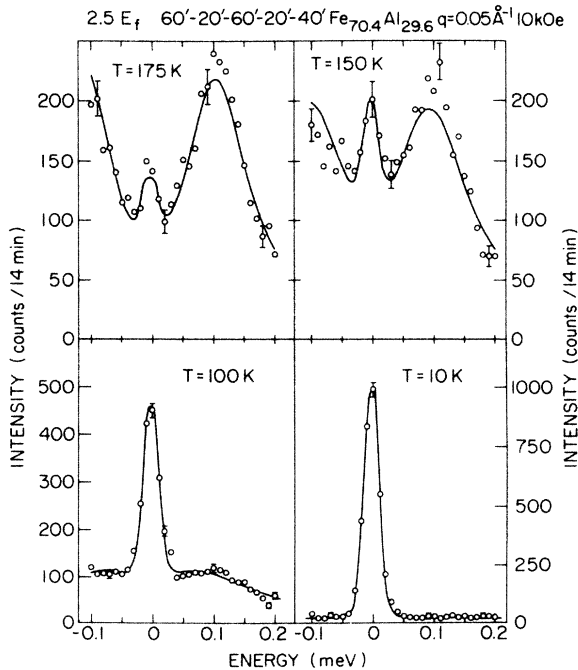


FIG. 5. Temperature dependence of the scattering at $q=0.05 \text{ \AA}^{-1}$ obtained in a horizontal field of 10 kOe. The solid lines are fits to $S_L(Q,E)$.

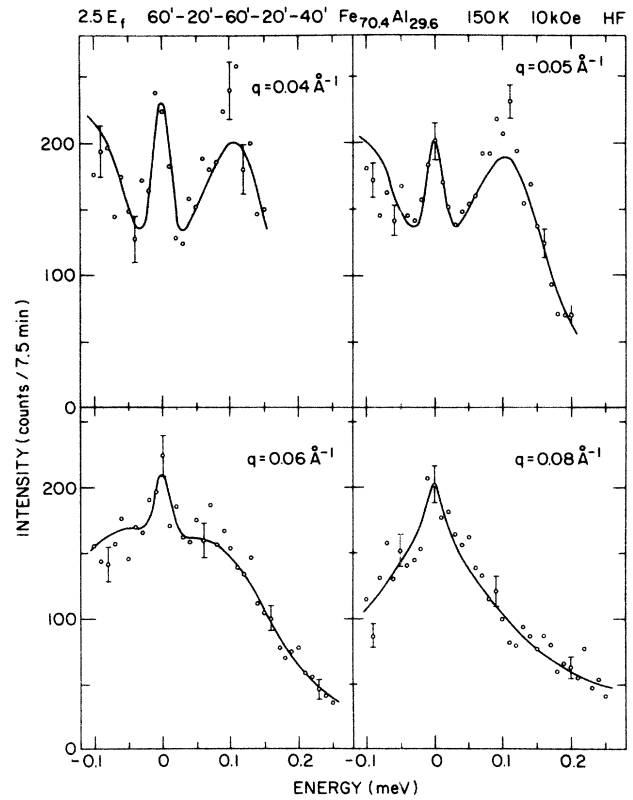


FIG. 7. Q dependence of the scattering at 150 K and 10 kOe. The solid lines are fits to $S_L(Q,E)$. The elastic peak is due to incoherent scattering and due to contamination by the direct beam and is not of magnetic origin.

laws can no longer be satisfied. The peaks broaden with increasing field and their intensity decreases. The amplitude of the elastic peak decreases also with increasing field which demonstrates that at least part of the intensity at $E = 0$ meV is of magnetic origin.

In Fig. 7 we show the q dependence of the scattering at 150 K in a horizontal field of 10 kOe. The relatively sharp peaks observed at small q broaden and move to smaller energies with increasing q . At $q = 0.08 \text{ \AA}^{-1}$ they have vanished and the scattering becomes diffusive. The elastic peak at $E = 0$ meV is of nonmagnetic origin (direct beam, incoherent scattering), in contrast to the measurements presented in Fig. 6 (VF), where at least part of the scattering around $E = 0$ meV is of magnetic origin.

The profile of the inelastic spectra depend on the direction of the field with respect to Q . Figure 8 shows that the peaks occur at larger Q and are broader in a vertical field than in a horizontal field. In the latter case there is only a nonmagnetic peak present at $E = 0$ meV, whereas in a VF, there is some magnetic, resolution-limited intensity at $E = 0$ meV, which is field dependent (see Fig. 6 and inset of Fig. 8). Since we observe only transverse and no longitudinal-spin fluctuations in HF, the elastic magnetic intensity in the VF is mainly due to

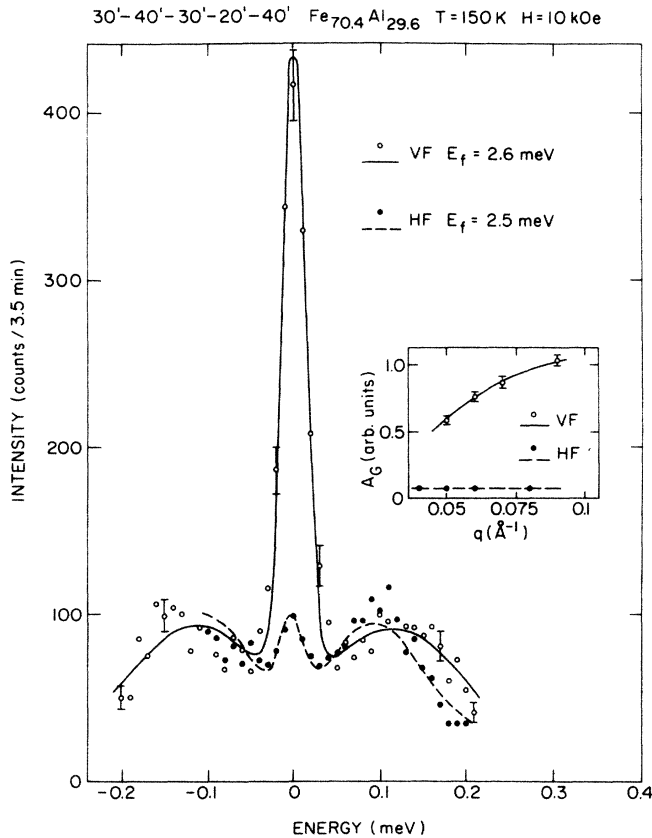


FIG. 8. Comparison of the scattering for $q = 0.05 \text{ \AA}^{-1}$ in a vertical and in a horizontal field. The inelastic scattering is apparently not isotropic. Solid lines are fits to $S_L(Q, E)$. The inset shows the q dependence of the elastic amplitude A_G . In a vertical field it is partly due to magnetic scattering.

longitudinal-spin fluctuations. A longitudinal contribution was also deduced from small-angle neutron scattering (SANS) studies on $\text{Ni}_{1-x}\text{Mn}_x$, $\text{Au}_{1-x}\text{Fe}_x$, and $(\text{Fe}_{1-x}\text{Mn}_x)_{75}\text{P}_{16}\text{B}_6\text{Al}_6$ by Hennion *et al.*,¹⁶ but in these experiments they could not discriminate between elastic and inelastic scattering.

In Fig. 9 we present E_q versus q^2 for different temperatures in a horizontal field of 10 kOe [Fig. 9(a)] and in a vertical field [Fig. 9(b)] at 150 K for both types of scattering $S_L(Q, E)$ and $S_{\text{DHO}}(Q, E)$. The result is truly remarkable: The slope of the dispersion curve changes sign below 200 K when the Lorentzian scattering function is used. The spin excitations exhibit a negative stiffness. The gap energy $\Delta = 0.11$ meV at $q = 0 \text{ \AA}^{-1}$, a value close to the Zeeman splitting $g\mu_B H$, is independent of temperature within the accuracy of our data [Fig. 9(a)]. If we assume the damped harmonic oscillator form $S_{\text{DHO}}(Q, E)$, we obtain always a dispersion curve with a positive slope. The gap energy increases always with increasing field. Since β_q and E_q become strongly correlated at large q and only one single peak around $E = 0$ meV is observed at large q (Fig. 7, $q = 0.08 \text{ \AA}^{-1}$), we believe that the positive slope of the dispersion curve at low temperature is just an artifact of the over-damped harmonic oscillator function. A detailed

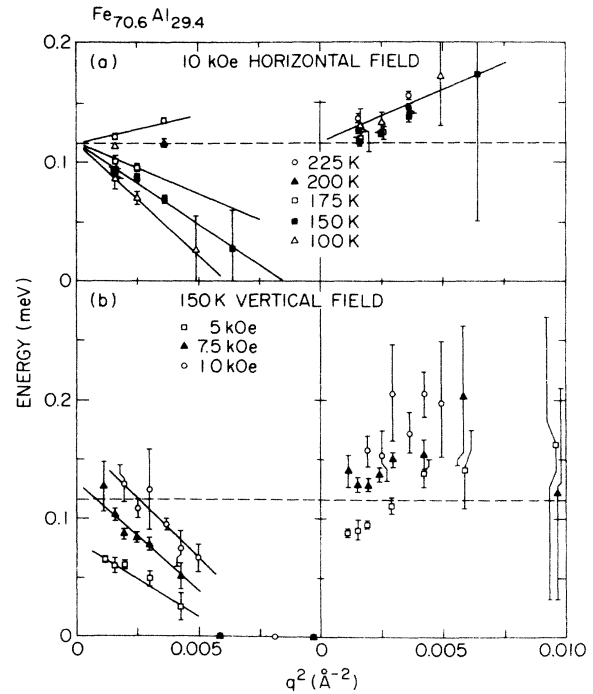


FIG. 9. (a) Temperature and (b) field dependence of the spin-wave energy in horizontal and vertical fields resulting from fits to a Lorentzian (left) and a damped harmonic oscillator (right). In the former case we observe a “negative” dispersion. Solid lines are guides to the eye. The dashed horizontal lines indicate the Zeeman energy $g\mu_B H$ for $H = 10$ kOe and $g = 2$.

analysis also shows that the linewidths increase rapidly with decreasing temperature, increasing field, and increasing q .

IV. DISCUSSION

The present field-dependent neutron scattering results of the RSG $\text{Fe}_{70.4}\text{Al}_{29.6}$ differ substantially from similar but less extensive measurements in the spin-glass phase of the RSG $\text{Fe}_x\text{Cr}_{1-x}$ (Ref. 14). Although the spins are aligned along the field direction in both systems under an applied field of several kOe, no spin waves are discernible in the spin-glass phase of $\text{Fe}_{70.4}\text{Al}_{29.6}$, in marked contrast to $\text{Fe}_x\text{Cr}_{1-x}$, where spin waves with a similar dispersion as in the ferromagnetic state are induced.^{14,19} The spin-wave peaks in $\text{Fe}_{70.4}\text{Al}_{29.6}$ move toward smaller energy for fixed Q with decreasing temperature. At 10 K we do not observe any inelastic scattering. There are at least two possibilities (besides experimental limitations), why we observe no spin waves at 10 K: (i) the spin waves are very heavily damped in the investigated q range and cannot be detected with our instrument, or (ii) spin waves cease to exist in the induced ferromagnetic state. For both scenarios the field-induced state in $\text{Fe}_{70.4}\text{Al}_{29.6}$ must be very soft for spin-wave excitations when compared with $\text{Fe}_x\text{Cr}_{1-x}$. One may speculate that the different dynamic behavior is caused by the different kind of diluting atoms, although neither Al (Ref. 6) nor Cr (Ref. 14) carries a magnetic moment, when alloyed in Fe. However, $\text{Fe}_{70.4}\text{Al}_{29.6}$ exhibits an intermediate paramagnetic phase which decouples the ferromagnetic state from the spin-glass state at low temperatures, in contrast to $\text{Fe}_x\text{Cr}_{1-x}$, where the ferromagnetic state transforms directly into the spin-glass state.

The rest of this section is devoted to a discussion of the most important result of the present study, the observation of a "negative" dispersion curve under an applied field at temperature below 200 K. There are several mechanisms which may explain our observations and we discuss in the following some of these.

We have recently reported about a field-induced modulated structure in the present sample.¹⁵ In a field of 10 kOe an elastic peak appears at $q_0 = 0.1 \text{ \AA}^{-1}$ in the spin-glass phase [in contrast to $\text{Fe}_x\text{Cr}_{1-x}$ (Ref. 19)] which we interpreted in terms of a modulated spin structure. Figure 9 shows that the q dependences of the Lorentzian peak positions extrapolate to zero energy near $q^2 \approx 0.01 \text{ \AA}^{-2}$, which corresponds roughly to q_0^2 . Therefore the intersection of the dispersion curves with the q^2 axis could be interpreted as a field-induced zone center caused by the underlying modulation. This interpretation is not consistent with the experimental observation, however, because (i) the spin wave should be sharp near the zone center, and (ii) from the temperature dependence of q_0 we would expect the zone center to move to smaller q with increasing temperature, in disagreement with Fig. 9.

The neutron scattering measurements⁶⁻⁸ of $\text{Fe}_{70.4}\text{Al}_{29.6}$ indicate that the intermediate paramagnetic phase (in zero field) is composed of correlated ferromagnetic clusters which are randomly oriented [Fig. 10(b)].

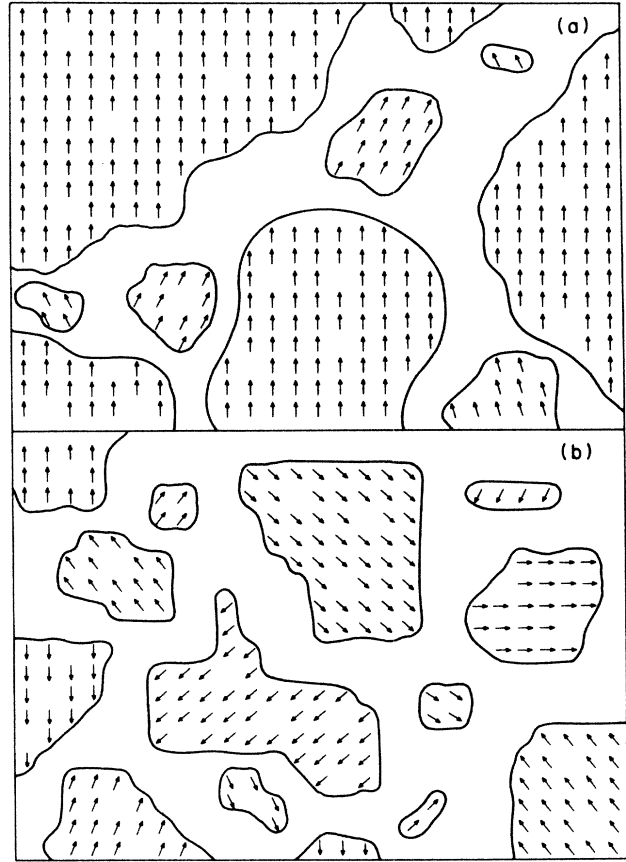


FIG. 10. Simple model for the spin configuration in the spin-glass phase or the superparamagnetic phase of $\text{Fe}_{70.4}\text{Al}_{29.6}$ in (a) a vertical field and in (b) a zero field. The spins in between the clusters are assumed to be oriented randomly. Their orientation freezes in with decreasing temperature and starts dissolving the ferromagnetic clusters. When a field is applied, then the bigger clusters align parallel to the field and grow in size. The smaller clusters are less aligned and exhibit characteristic transverse correlations.

The linewidth of the quasielastic scattering is a measure of the lifetime of these clusters. Under an applied field the larger clusters align first along the field direction and grow in size [Fig. 10(a)] maintaining characteristic transverse correlations which give rise to the elastic peak at finite Q . When a spin wave with a long wavelength propagates through the sample, then the spins of large clusters, which are oriented almost parallel to the field, have to be reversed against the external field H . Therefore we expect at $q=0$ a temperature-independent gap in the energy spectrum of the order of $g\mu_B H$. Spin waves at larger q involve the reversing of smaller spin clusters. The spins in these clusters are not parallel to \mathbf{H} because the competing exchange interactions are more important (the surface-to-volume ratio is smaller) and it affords less energy to reverse the spins in such clusters. Therefore the dispersion curve has a negative slope which depends on temperature, since the cluster size decreases with decreasing temperature. A similar interpretation has been given by Carlson *et al.*²⁰ to explain the

observed field-induced negative dispersion in the diluted amorphous antiferromagnet n -type CdS.

According to the above model, we expect a decrease in energy with increasing q and decreasing field (Fig. 9). Because the exchange interactions are sensitive to stoichiometry the spin-wave energy is not uniquely defined. Moreover, the peaks exhibit an additional broadening due to small-scale concentration fluctuations as observed in the experiment. This effect is more important at lower temperatures, hence, we expect a steeper negative slope of the dispersion curve, until at 10 K the inelastic scattering has vanished completely in the q range investigated.

Finally, we discuss the observed anisotropy of the inelastic scattering in Fig. 8. Let us define as z axis the direction of the magnetic field, as y axis the direction perpendicular to the plane defined by the two field configurations (HF and VF), and the x axis normal to y and z . In a horizontal field we observe transverse-spin fluctuations (spin waves) $\langle S_x \rangle$ and $\langle S_y \rangle$ since $\mathbf{H} \parallel \mathbf{Q}$. When we apply a vertical field, then we observe again the transverse fluctuations $\langle S_y \rangle$ as before, and longitudinal fluctuations (with respect to H) $\langle S_z \rangle$ which, as we mentioned above, contribute to the elastic scattering. Because of the different profiles of the inelastic peaks in HF and VF (Fig. 8), respectively, $\langle S_z \rangle$ must exhibit peaks at finite energy too, in order to pull the peak posi-

tion further away from $E=0$ meV. Since the spectra have been measured with two different experimental setups, it is not possible to determine the exact profile of $\langle S_z \rangle$. This topic will be investigated later. The different profiles may be connected with the onset of freezing of the transverse-spin components in an applied field as predicted by Gabay and Toulouse.⁵

The inelastic neutron scattering from the spin dynamics in $\text{Fe}_{70.4}\text{Al}_{29.6}$ shows a very complicated behavior when a magnetic field is applied. We hope that similar measurements are extended to smaller Q and E in order to test the above conjectures. The field dependence of the ground state in $\text{Fe}_{70.4}\text{Al}_{29.6}$ differs from the ground state in the RSG $\text{Fe}_x\text{Cr}_{1-x}$.

ACKNOWLEDGMENTS

We would like to thank J. Schefer and D. Schneider for helping us to use the small-angle neutron scattering instrument and the analysis of the SANS data. We appreciate fruitful discussions with S. Geschwind and W. M. Saslow. This work was supported by the Division of Material Sciences, U.S. Department of Energy under Contract No. DE-AC02-76CH00016, and carried out as a part of the U.S.-Japan Cooperative Neutron Scattering Program.

¹C. Y. Huang, *J. Magn. Magn. Mater.* **51**, 1 (1985).

²K. H. Fischer, *Phys. Status Solidi B* **116**, 387 (1983); **130**, 13 (1985).

³I. A. Campbell, *Phys. Rev. B* **33**, 3587 (1986).

⁴M. Continentino and A. P. Malozemoff, *Phys. Rev. B* **34**, 471 (1986).

⁵M. Gabay and G. Toulouse, *Phys. Rev. Lett.* **47**, 201 (1981).

⁶J. W. Cable, L. David, and R. Parra, *Phys. Rev. B* **16**, 1132 (1977).

⁷H. R. Child, *J. Appl. Phys.* **52**, 1732 (1981).

⁸K. Motoya, S. M. Shapiro, and Y. Muraoka, *Phys. Rev. B* **28**, 6183 (1983).

⁹B. Hennion, M. Hennion, F. Hippert, and A. P. Murani, *J. Phys. F* **14**, 489 (1984).

¹⁰M. L. Spano, H. A. Alperin, J. J. Rhyne, S. J. Pickart, S. Hasanain, and D. Andrauskas, *J. Appl. Phys.* **57**, 3432 (1985).

¹¹J. J. Rhyne and C. J. Glinka, *J. Appl. Phys.* **55**, 1691 (1984).

¹²S. J. Pickart, S. Hasanain, D. Andrauskas, H. A. Alperin, M. L. Spano, and J. J. Rhyne, *J. Appl. Phys.* **57**, 3430 (1985).

¹³D. Boumazouza, C. Tete, J. Durand, Ph. Mangin, and J. L. Soubeyroux, *J. Magn. Magn. Mater.* **54-57**, 95 (1986).

¹⁴S. M. Shapiro, C. R. Fincher, A. C. Palumbo, and R. D. Parks, *Phys. Rev. B* **24**, 6661 (1981).

¹⁵P. Böni, S. M. Shapiro, and K. Motoya, *Solid State Commun.* **60**, 881 (1986).

¹⁶M. Hennion, I. Mirebeau, F. Hippert, B. Hennion, and J. Bigot, *J. Magn. Magn. Mater.* **54-57**, 121 (1986); M. Hennion, I. Mirebeau, B. Hennion, S. Lequien, and F. Hippert, *Europhys. Lett.* **2**, 393 (1986); and S. Lequien, I. Mirebeau, M. Hennion, B. Hennion, F. Hippert, and A. P. Murani, *Phys. Rev. B* **35**, 7279 (1987).

¹⁷G. L. Squires, *Introduction to the Theory of Thermal Neutron Scattering* (Cambridge University Press, Cambridge, 1978).

¹⁸M. F. Collins, V. J. Minkiewicz, R. Nathans, L. Passell, and G. Shirane, *Phys. Rev.* **179**, 417 (1969).

¹⁹P. Böni and S. M. Shapiro, *Bull. Am. Phys. Soc.* **32**, 630 (1987).

²⁰N. W. Carlson, S. Geschwind, L. R. Walker, and G. E. Devlin, *Phys. Rev. Lett.* **49**, 165 (1982).